# Identification of a novel *MYO1F::MLLT10* fusion in adult acute monocytic leukemia

Acute myeloid leukemia (AML) is a heterogeneous malignancy characterized by clonal proliferation of myeloid precursors, often driven by recurrent cytogenetic and molecular abnormalities. Translocations involving the *KMT2A* (MLL) gene at 11q23.3 occur in AML, particularly in infant and pediatric cases, and are associated with monocytic differentiation and poor prognosis.[1-3] The *MLLT10* gene at 10p12.31, a frequent *KMT2A* fusion partner, is implicated in AML and T-cell acute lymphoblastic leukemia (T-ALL) with monocytic features.[3,4] *MYO1F* at 19p13.2, encoding an unconventional myosin protein, is a rare *KMT2A* fusion partner reported in a few infant and pediatric AML cases (2 infants with *KMT2A::MYO1F*, 1 with a complex rearrangement and 1 pediatric case with a complex translocation involving chromosomes 7, 11, 19, and 22).[1,2,5,6] To our knowledge, *MYO1F::MLLT10* fusion has not previously been described in AML. We report the first adult case of acute monocytic leukemia (World Health Organization/International Consensus Classification 2022) with reciprocal in-frame *MYO1F::MLLT10* and *MLLT10::MYO1F* fusions, identified by RNA sequencing and supported by interphase fluorescence *in situ* hybridization (FISH).

A 58-year-old man with diabetes mellitus, chronic kidney disease, hypertension, and renal stones presented with right lower quadrant abdominal pain, nausea, vomiting, and fatigue. Imaging revealed left staghorn calculus, atrophic right kidney, splenic infarct, hepatosplenomegaly, and non-bulky multi-station lymphadenopathy. Laboratory findings revealed rapidly progressive leukocytosis (white blood cell count [WBC] 33.7x$10^9$/L initially, rising to 104x$10^9$/L pre-percutaneous nephrostomy [PCN]), anemia (hemoglobin [Hb] 8 g/dL), thrombocytopenia (platelets 128x$10^9$/L), and acute kidney injury. Bone marrow aspiration and biopsy demonstrated a markedly hypercellular marrow (>95%) with >80% blasts/blast equivalents. Flow cytometry confirmed 73% blasts, positive for CD117, HLA-DR, CD11b, CD11c, CD13, CD15, CD33, CD38, partial CD14 and CD64, and negative for CD34, CD19, TdT, MPO. Abnormal monocytes (11%) expressed CD56 with decreased CD14. Peripheral smear revealed predominantly monoblasts and promonocytes with characteristic cytomorphology.

Bone marrow cells cultured for 24 hours revealed a karyotype of 45,X,-Y/46,XY (75% of cells with -Y), confirmed by chromosomal microarray analysis (-Y in ~70% of cells). Standard FISH was negative for common AML rearrangements (*MECOM*, *DEK::NUP214*, *RUNX1T1::RUNX1*, *BCR/ABL1*, *KMT2A*, *PML/RARA*, and *CBFB*) and *TP53* deletion. Next-generation sequencing (NGS)-based targeted DNA sequencing (275-gene panel) revealed no pathogenic mutations, including *FLT3*-internal tandem duplication (ITD)/*TKD* or *NPM1*, with a low tumor mutation burden (2.4 mutations/Mb). RNA fusion panel (TruSight 507-gene panel) detected two novel in-frame chimeric fusion transcripts: *MYO1F::MLLT10* and *MLLT10::MYO1F* (Figures 1 and 2). Metaphase spreads lacked a discernible t(10;19)(p12.31; p13.2). Therefore, an *MLLT10/KMT2A* dual fusion probe on destained G-banded metaphase spreads (Figure 3A, B), showed *MLLT10* signals only on chromosome 10 short arms; no signals on either chromosome 19. However, 49% of interphase nuclei (98/200) displayed three *MLLT10* signals - one large, two smaller - often close together (82/98 nuclei, 83.7%; Figure 3C) - indicating a split *MLLT10* allele, potentially involving an insertion of *MYO1F* sequences from 19p13.2 into the *MLLT10* gene region at 10p12.31, suggesting *MLLT10* rearrangement. Initial management included leukapheresis (WBC reduced to 39.3x$10^9$/L) and hydroxyurea (1 g twice a day for 4 days), followed by azacitidine/venetoclax (ven) induction (7+21 days, VIALE-A protocol). The patient had a partial response, but persistent disease (20% blasts) on bone marrow biopsy 2 weeks later. He later received FLAG-IDA-Ven salvage therapy and achieved short-lived complete remission. He relapsed (43% blasts, WBC 183.6x$10^9$/L) 3 weeks after first consolidative high-dose cytarabine (HiDAC) (~4 months from the diagnosis) and was treated with leukapheresis (×2) and hydroxyurea. At the latest follow-up, 2 weeks post-relapse, he was on supportive care only, without AML-directed therapy, amid multiorgan failure (renal, ocular), awaiting hospice care.

The biospecimens and clinical data used in this study were collected previously as part of the patient's routine diagnostic work-up and clinical care. No separate specimens were collected for the study. The institutional review board of Fox Chase Cancer Center provided ethical approval for this work.

This case represents the first report of *MYO1F::MLLT10* and reciprocal *MLLT10::MYO1F* fusions in AML (*Online Supplementary Table S1*), identified by RNA sequencing, confirmed by multiple fusion-calling algorithms (using FusionCatcher, STAR-Fusion, and Arriba; *Online Supplementary Table S2*), and supported by orthogonal testing using FISH (Figure 3A-C). *MLLT10* (also known as *AF10*), a known fusion partner in AML and T-ALL (e.g., *KMT2A::MLLT10*, *PICALM::MLLT10*), drives leukemogenesis via its 3' domains (plant homeodomain [PHD]-finger, leucine zipper), promoting monocytic differentiation through chromatin remodeling and transcriptional dysregulation (e.g., DOT1L recruitment, H3K79 methylation).[3,4] In *MYO1F::MLLT10* fusion protein (443 amino acids [aa]), *5' MYO1F* exon 1 (start codon, promoter/enhancer elements) fuses to the C-terminal exons

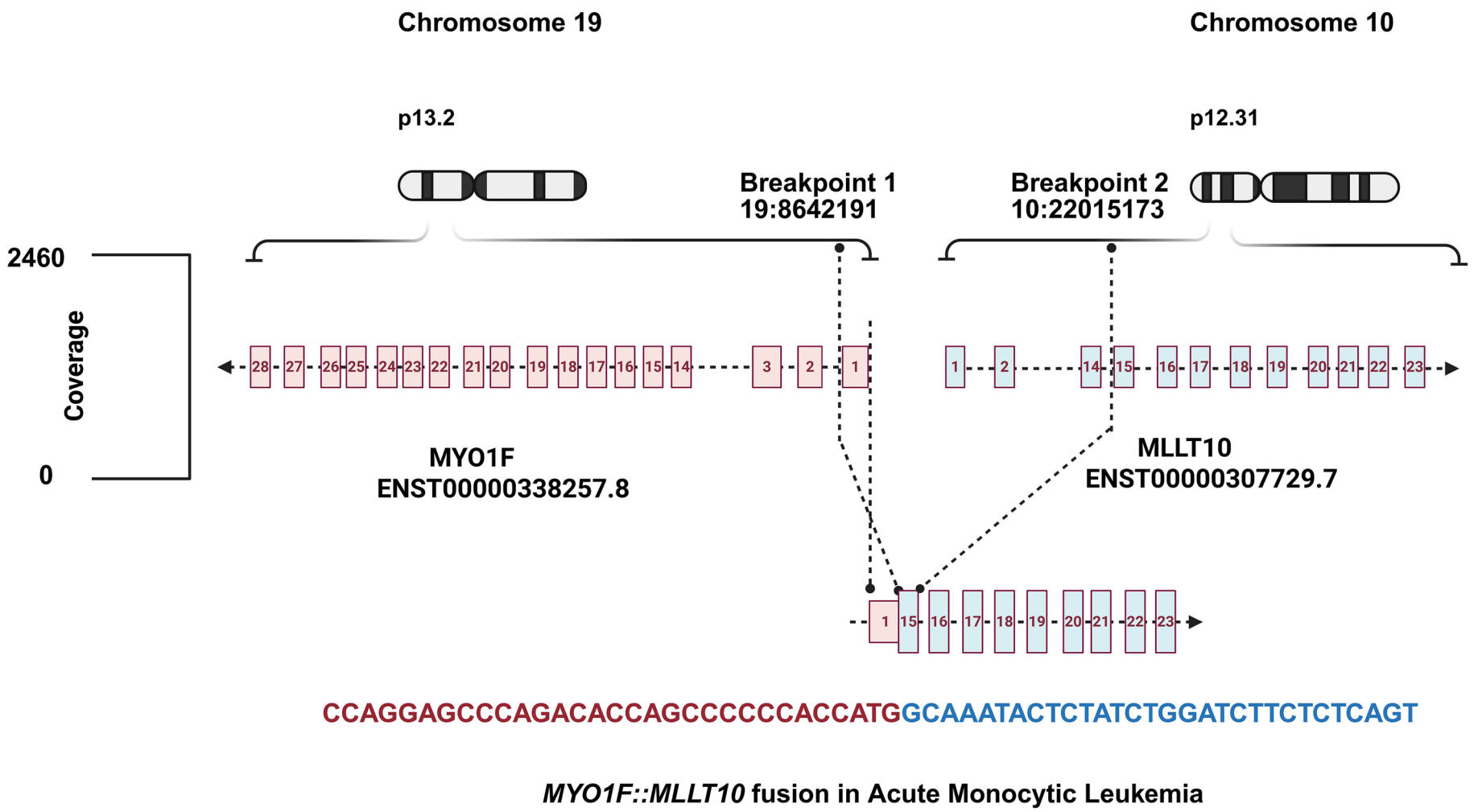


**Figure 1. Schematic of *MYO1F::MLLT10* fusion in acute monocytic leukemia.** This diagram illustrates the *MYO1F::MLLT10* fusion generated by a chromosomal rearrangement between 10p12.31 and 19p13.2. The breakpoint in the *MYO1F* occurs at chr19:8642191 (exon 1, start codon, negative strand) from chromosome 19, which fuses to the *MLLT10* gene at chr10:22015173–22015284 (exon 15/16, positive strand). The resulting in-frame chimeric transcript, confirmed by RNA sequencing, encodes a protein that combines promoter/enhancer elements and the start codon of *MYO1F* with the transcriptional regulatory domains of *MLLT10*, driving acute monocytic leukemia. Exons are represented as boxes, introns as lines, and the fusion junction is indicated by a dashed line. Chromosomal orientations and breakpoints are annotated for clarity.

15–23 (442 aa) of the *3' MLLT10* partner, potentially up-regulating *MLLT10's* oncogenic domains. In the reciprocal MLLT10::MYO1F fusion protein (839 aa), *5' MLLT10* exons 1-18 (816 aa; N-terminal domains including PHD-finger, zf-HC5HC2H) fuses to *3' MYO1F* exons 25-28 (23 aa, partial myosin tail). The *MYO1F::MLLT10* fusion transcript (breakpoints: *5′ MYO1F*, chr19:8,642,191 [– strand]; *3′ MLLT10*, chr10:22,015,173 [+ strand]) showed high expression levels and strong read support: STAR-Fusion (62 fragments: 39 junction, 23 spanning; FFPM=13.4276), FusionCatcher (61 fragments: 19 unique, 42 spanning), and Arriba (42 fragments: 6/27 split reads, 9 discordant mates). The fusion maintains the reading frame and encodes a chimeric protein (MANTLSGSS..., 443 aa; *Online Supplementary Table S1*). The reciprocal *MLLT10::MYO1F* fusion (breakpoints: *5′ MLLT10*, chr10:22,022,016 [+ strand]; *3′ MYO1F*, chr19:8,590,446 [– strand]) was detected by STAR-Fusion (43 fragments: 40 junction reads, 3 spanning; FFPM=9.3126), FusionCatcher (54 fragments: 12 unique reads, 42 spanning pairs), and Arriba (24 fragments: 14/8 split reads, 2 discordant mates; coverage 309/85). This chimeric transcript was predicted to be in-frame according to STAR-Fusion and FusionCatcher, but out-of-frame according to Arriba due to selection of a shorter *MYO1F* isoform (507 bp in ENST00000596245.1 *vs*. 4,303 bp in ENST00000338257.8). It encodes a chimeric fusion protein (MVSSDR..., 839 aa; *Online Supplementary Table S1*). STAR-Fusion and FusionCatcher confirm canonical GT/AG splice sites for both fusions with Arriba's CDS/splice site annotations reflecting minor junction mapping differences. High expression levels (FFPM 13.4276 for *MYO1F::MLLT10 vs*. 9.3126 for *MLLT10::MYO1F*) and Arriba's coverage support *MYO1F::MLLT10* as the driver (*Online Supplementary Table S2*), with C-terminal domains of 3' *MLLT10* driving leukemogenesis, akin to *KMT2A::MLLT10* fusions. In the reciprocal *MLLT10::MYO1F* fusion, the retained N-terminal PHD-finger and SH3 domains from 5′ *MLLT10* suggest potential functionality with a secondary regulatory role, possibly contributing to stabilization of the rearrangement/translocation; however, it may be less oncogenic due to the lack of C-terminal oncogenic leucine zipper. Only 23 aa (part of the myosin tail) from 3' exons 25-28 of *MYO1F* are included, indicating truncation of the fusion protein by a stop codon (EPTRKGMAKGKPRRSSQAPTRAA*) and translation of only part of *MYO1F* exon 25 sequence (chr19:8590446 to 8590363 [- strand], 84bp, 28 aa). This region lacks significant functional domains (e.g., the motor domain encoded by earlier exons), suggesting a primarily

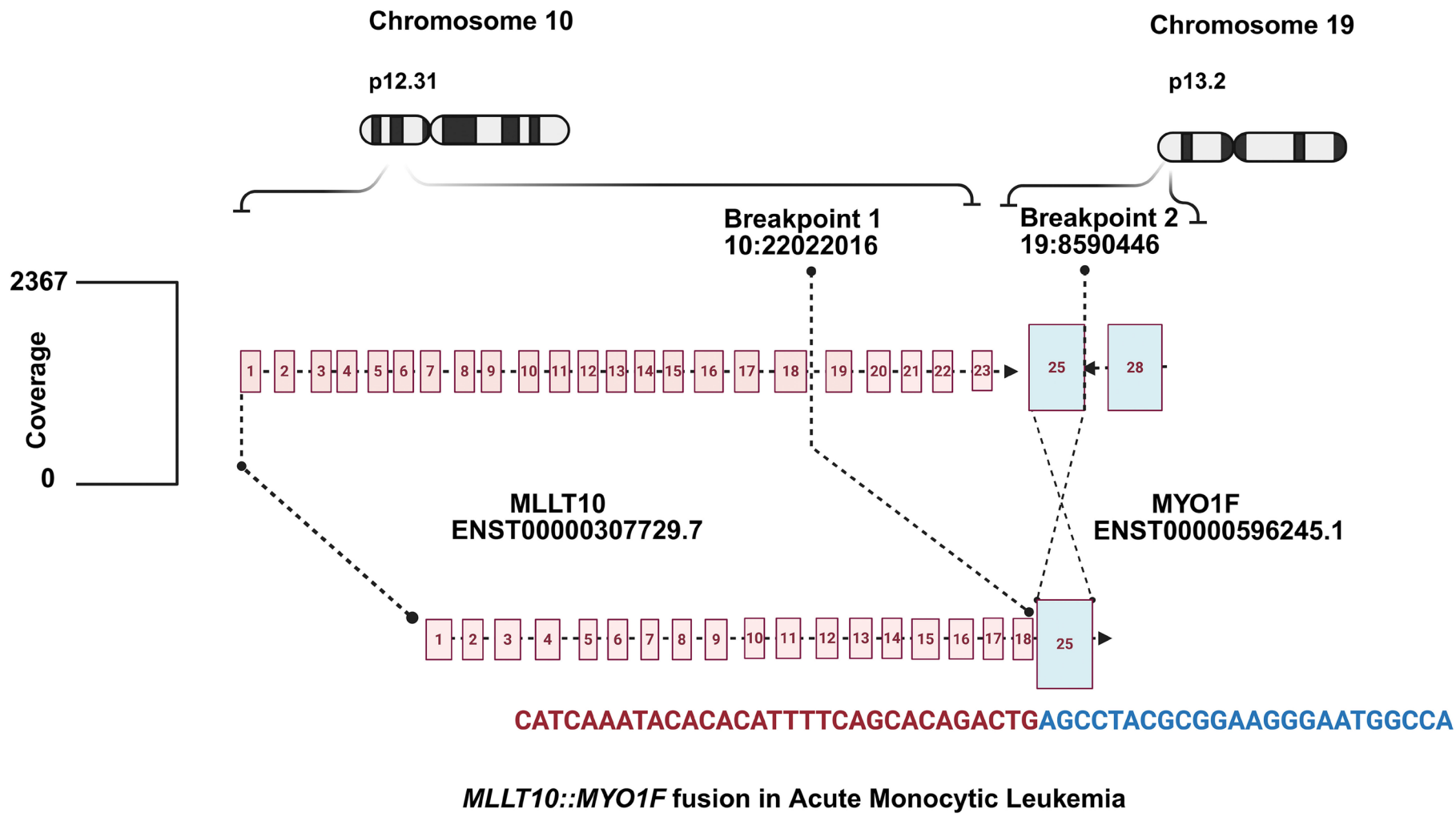


**Figure 2. Schematic of *MLLT10::MYO1F* fusion in acute monocytic leukemia.** This diagram shows *MLLT10::MYO1F* reciprocal fusion from the same chromosomal translocation. The breakpoint in the *MLLT10* is at chr10:22022016 (exon 18/19, positive strand), retaining regulatory domains including the plant homeodomain (PHD)-finger, zinc finger (zf)-HC5HC2H, and Jnk-SapK_ap motifs, which fuses to the *MYO1F* at chr19:8590363-8590446 (exon 25, negative strand). RNA sequencing confirmed the fusion transcript, which combines the N-terminal region of *MLLT10* with the C-terminal exons of *MYO1F*, encoding an in-frame chimeric protein according to STAR-Fusion and FusionCatcher and an out-of-frame protein according to Arriba. While *MLLT10's* retained regulatory domains may contribute to fusion stability or minor functions, the fusion likely has reduced oncogenic potential. Exons are represented as boxes, introns as lines, and the fusion junction is indicated by a dashed line. Chromosomal orientations and breakpoints are annotated for clarity.

structural rather than functional role in the fusion protein. The asymmetric breakpoints in *MLLT10* and *MYO1F* in both fusion products likely indicate an unbalanced reciprocal translocation. However, the presence of *MLLT10* exons 15-18 in both derivative chromosomes raises the possibility of a duplicated segment and thus cannot entirely exclude a complex rearrangement from additional events. FISH with an *MLLT10/KMT2A* probe showed no detectable *MLLT10* signal splitting in metaphase spreads (limited by suboptimal banding quality and insufficient metaphase spreads), but 49% of interphase nuclei displayed three *MLLT10* signals (1 large, 2 smaller), indicating a split *MLLT10* allele, likely due to a cryptic insertion of *MYO1F* sequences from 19p13.2 into the *MLLT10* gene at 10p12.31. Interphase FISH confirmed the *MLLT10* rearrangement, while the absence of visible chromosomal alterations suggests a submicroscopic cryptic insertion or underrepresentation of the malignant clone in metaphase spreads. The cryptic nature of the 10p;19p rearrangement, without other AML-defining cytogenetic changes, highlights the value of RNA fusion analysis for identifying rare gene fusions.

*MYO1F*, a rare *KMT2A* partner in infant AML, may contribute to cytoskeletal or signaling abnormalities, a novel role when fused with *MLLT10*.[5,6] The *MYO1F::MLLT10* fusion in this case is likely driving the monocytic phenotype (>80% blasts, CD117$^{+}$, CD34$^{-}$, CD56$^{+}$, partial CD14$^{+}$), consistent with *MLLT10*-rearranged AML.[3,4] Although the absence of *FLT3/NPM1* mutations was favorable, the relapse after first consolidative HiDAC indicates poor prognosis.[7] The patient's complex clinical course, including retinal hemorrhages and renal failure, underscores the systemic impact of AML.

This case expands the spectrum of *MLLT10* rearrangements in AML and contributes to the evolving understanding of rare AML-associated fusions. Its identification by targeted RNA sequencing - with robust read support, high expression, and in-frame predictions across multiple fusion calling algorithms - underscores the importance of integrated molecular and cytogenetic profiling in AML. Because *MYO1F::MLLT10* was identified only through RNA sequencing, similar cryptic events may currently be under-recognized. Broader screening of AML cohorts using targeted RNA sequencing or polymerase chain reaction analysis of cDNA

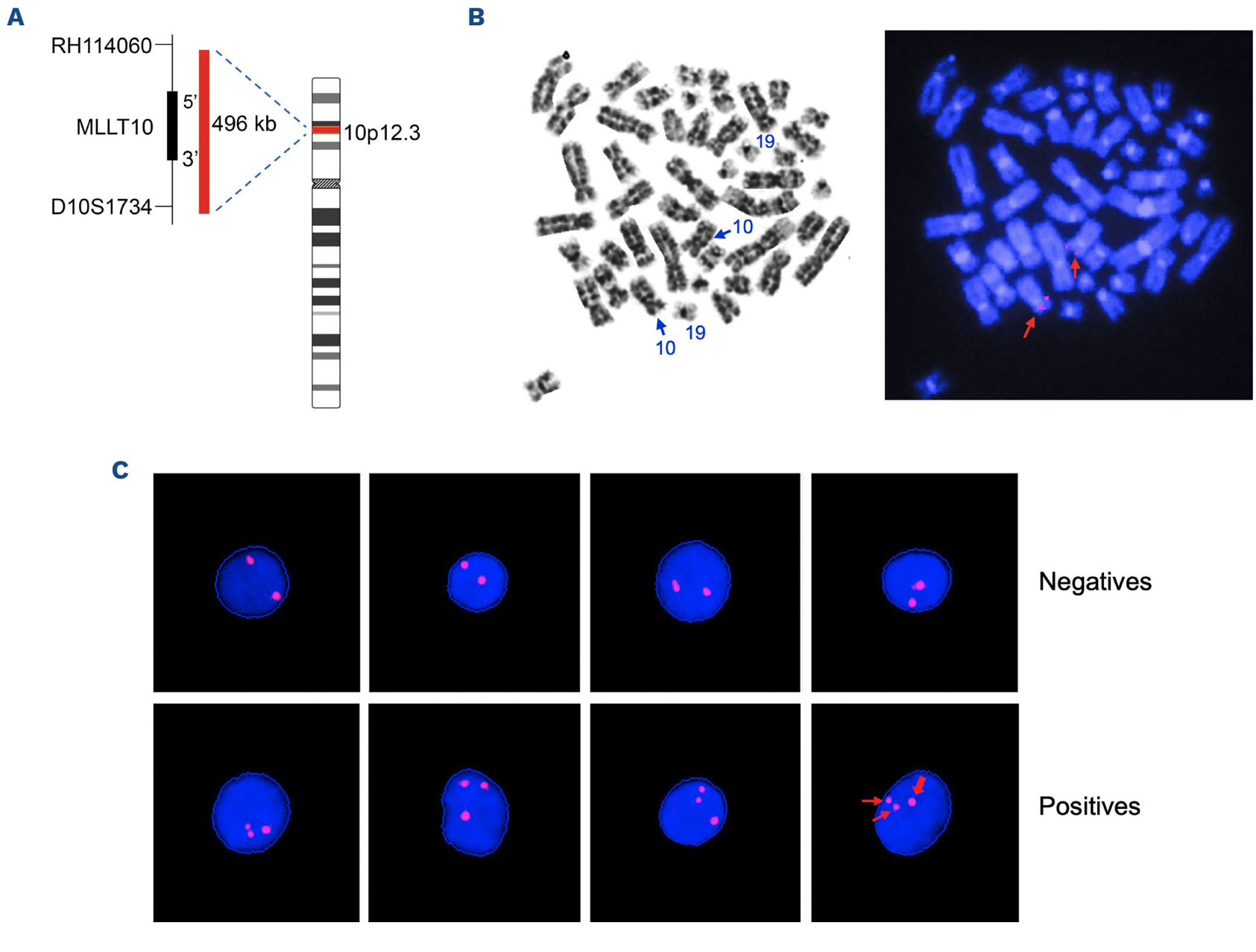


**Figure 3. Hybridization of *MLLT10* probe in patient bone marrow cells.** (A) Schematic of orange-labeled *MLLT10* probe hybridizing to the entire *MLLT10* locus and flanking sequences at sub-band 10p12.3 (adapted from the MetaSystems XL t(10;11) *MLLT10/KMT2A* Dual Fusion Probe [MetaSystems, Medford, MA]), which comprises an orange-labeled probe targeting the *MLLT10* gene region at 10p12.31 and a green-labeled probe targeting the *KMT2A* gene region at 11q23.3; the latter probe is not shown). (B) G-banding (left) and hybridization of *MLLT10/KMT2A* probe (right) to a representative 4′,6-diamidino-2-phenylindole (DAPI)-stained metaphase spread from the patient's bone marrow. The *MLLT10* probe hybridizes to the short arm of chromosome 10 only (red arrows), with no hybridization to chromosome arm 19p (100x objective lens; total magnification of 160x). (C) Representative fluorescence *in situ* hybridization (FISH) images showing nuclei with: (top panel) normal two *MLLT10* signal pattern; (bottom panel) abnormal pattern, exhibiting 1 larger *MLLT10* signal (thick vertical arrow on far right) and 2 smaller *MLLT10* signals (thin red arrows in same nucleus) (20x objective lens; total magnification of 32x). Images of interphase nuclei were captured using a MetaSystems Metafer microscope workstation, and the raw images were extracted and processed to depict *MLLT10* signals in magenta and DAPI-stained nuclei in blue, with blue outlines marking nuclear boundaries.

from diagnostic bone marrow aspirates will be essential to ascertain its prevalence. The *MYO1F::MLLT10* fusion is the probable leukemogenic driver, analogous to *KMT2A::MLLT10* or cytoskeletal perturbations from *MYO1F's* functional domains. In line with the approaches for novel fusion genes such as *NUP98-NSD1*, the transforming activity of *MYO1F::MLLT10* can be assessed using *in vitro* assays - including foci formation or anchorage-independent growth by transfection of a plasmid expressing *MYO1F::MLLT10* into NIH-3T3 fibroblasts. Additional insights could be obtained by evaluating proliferation rates and/or altered differentiation in normal or immortalized myeloid cell lines.[8] Furthermore, assessing therapeutic vulnerabilities - such as to *DOT1L* inhibitors that target chromatin-remodeling pathways implicated in *MLLT10*-driven malignancies - could reveal actionable targets for this rare AML subtype.

## Authors

Bhaumik Shah,[1] Roniya Francis,[1] Jianming Pei,[2] Ryan Neumann-Domer,[3] Nicholas Mackrides,[1] Joseph R. Testa[3,4] and Reza Nejati[1]

[1]Department of Pathology, Fox Chase Cancer Center, Temple University Health System; [2]Molecular Diagnostics Laboratory, Fox Chase Cancer Center; [3]Clinical Cytogenomics Laboratory, Fox Chase

Cancer Center and [4]Cancer Prevention and Control Program, Fox Chase Cancer Center, Philadelphia, PA, USA

Correspondence:
R. NEJATI - Reza.Nejati@fccc.edu

https://doi.org/10.3324/haematol.2025.288255

Received: May 22, 2025.
Accepted: November 7, 2025.
Early view: November 20, 2025.



**Disclosures**

No conflicts of interest to disclose.

**Contributions**

The original concept was developed by BS and JP. Diagnostic work-up was performed by BS, NM and RN. The literature review was conducted by BS and JP. Data collection and analysis were carried out by JP, JT, RN, RF and BS. Data interpretation was performed by JP, JT and BS. BS wrote the original draft of the manuscript. Critical review and editing were undertaken by BS, JP, JT, NM, RF and RN. All authors approved the final version of the manuscript and agree to be accountable for all aspects of the work.

**Data-sharing statement**

De-identified raw RNA-sequencing data supporting the identification of the *MYO1F::MLLT10 and MLLT10::MYO1F* fusions, together with a tab-separated valuesfile containing fusion gene details, breakpoints, read support, and transcript annotations generated using FusionCatcher, STAR-Fusion, and Arriba, are available upon reasonable request. These data can be obtained by contacting the corresponding author, subject to compliance with the institutional review board policies of Fox Chase Cancer Center to ensure patient confidentiality and ethical standards.

# References

1. Meyer C, Hofmann J, Burmeister T, et al. The MLL recombinome of acute leukemias in 2013. Leukemia. 2013;27(11):2165-2176.
2. Meyer C, Burmeister T, Gröger D, et al. The MLL recombinome of acute leukemias in 2017. Leukemia. 2018;32(2):273-284.
3. Meyer C, Kern W, Schnittger S, et al. The KMT2A recombinome of acute leukemias in 2023. Leukemia. 2023;37(5):988-1005.
4. Panagopoulos I, Andersen K, Eilert-Olsen M, et al. Rare KMT2A-ELL and novel ZNF56 - KMT2A fusion genes in pediatric T-cell acute lymphoblastic leukemia. Cancer Genomics Proteomics. 2021;18(2):121-131.
5. Duhoux FP, Ameye G, Libouton JM, et al. The t(11;19)(q23;p13) fusing MLL with MYO1F is recurrent in infant acute myeloid leukemias. Leuk Res. 2011;35(9):e171-e172.
6. Taki T, Akiyama M, Saito S, et al. The MYO1F, unconventional myosin type 1F, gene is fused to MLL in infant acute monocytic leukemia with a complex translocation involving chromosomes 7, 11, 19, and 22. Oncogene. 2005;24(33):5191-5197.
7. DiNardo CD, Lachowiez CA, Takahashi K, et al. Venetoclax combined with FLAG IDA induction and consolidation in newly diagnosed acute myeloid leukemia. Am J Hematol. 2022;97(8):1035-1043.
8. Thanasopoulou A, Tzankov A, Schwaller J. Potent co operation between the NUP98 NSD1 fusion and the FLT3 ITD mutation in acute myeloid leukemia induction. Haematologica. 2014;99(9):1465-1471.